Sarah Carmichael, James Seward, Bryce Norvell, Lucca Scoggins, Anna-Maria Riley, Morgan Smith, Howard Neufeld, and Suzanna Bräuer. The relationship between sediment geochemistry, manganese oxidation, human traffic, and microbial community structure across three southern Appalachian caves. *Journal of Cave and Karst Studies*, v. 88, no. 3, p. 45-61. DOI: 10.4311/2025MB0100

THE RELATIONSHIP BETWEEN SEDIMENT GEOCHEMISTRY, MANGANESE OXIDATION, HUMAN TRAFFIC, AND MICROBIAL COMMUNITY STRUCTURE ACROSS THREE SOUTHERN APPALACHIAN CAVES

Sarah Carmichael[1,C], James Seward[2], Bryce Norvell[3], Lucca Scoggins[1], Anna-Maria Riley[3], Morgan Smith[3,4], Howard Neufeld[3], and Suzanna Bräuer[3]

Abstract

Three southern Appalachian caves were assessed in a multiproxy analysis to determine if human visitation and modification of the cave environment could influence cave mineralogy, inorganic geochemistry, and microbial community assemblages. Cave sediments were collected from Daniel Boone Caverns in Fort Blackmore, VA (gated and locked with few visitors); Worley's Cave in Bluff City, TN (a wild show cave); and Linville Caverns outside of Marion, NC (a developed show cave). Sediments were all analyzed using Illumina sequencing for microbial community structure, as well as a combination of X-ray diffraction, whole-rock geochemistry, particle size distributions, and transmission electron microscopy (TEM) for mineral characterization. Distinct geochemical and microbial signatures were found both within and between the caves. Biological manganese oxidation was present in all three caves, with significant differences in geochemistry across sites that contained Mn oxides and those that did not. Geochemistry and mineralogy of sediments primarily reflected the local bedrock rather than human-associated traffic and detritus. PCA plots using whole-rock geochemistry (cross-referenced with X-ray diffraction data) indicate that sediment variability between caves was due to the amount of clay minerals relative to detrital feldspars and quartz, as well as the amount of detrital heavy minerals relative to Mn oxidation and phosphate. Sediment-hosted microbial communities from Linville Caverns (the most highly developed of the three caves) contained more Bacteroidota (a phylum associated both with high-molecular weight carbon and humans) than the other two caves, while Daniel Boone Caverns, a relatively pristine cave, contained more Thermoplasmatota, Chloroflexota, and Nitrospirota (oligotrophic phyla). Overall, our data corroborate studies demonstrating that Bacteroidota are positively correlated and Nitrospirota are negatively correlated with anthropogenic and nutrient input, and that bedrock type exerts a strong influence both on sediment geochemistry and on microbial community structure.

INTRODUCTION

Karst systems host vital sources of potable drinking water on a global scale (Hartmann et al., 2014) and support some of the most fragile and diverse ecosystems on Earth (Barton and Jurado, 2007; Engel, 2010; Brannen-Donnelly and Engel, 2015; Ma et al., 2021). Cave microorganisms are sensitive to variations in DOM from drip water (Cheng et al., 2024), flooding and sediment age (Mulec et al., 2025), artificial lighting (Mulec and Kosi, 2009; Burgoyne et al., 2021), and human visitation (Pronk et al., 2007, 2009; Bontemps et al., 2022). In particular, the anthropogenic impact in cave ecosystems has been globally documented (Zhong et al., 2011; Faimon et al., 2012; Saiz-Jimenez, 2012), and human visitation and the influx of human-derived materials can lead to the destruction of microhabitats (Northup, 2011), alteration of biogeochemical cycles, the introduction of fecal (Carmichael et al., 2013b) and skin-hosted (Biagioli et al., 2023) bacteria and fungi, the introduction of alien or invasive species (Nicolosi et al., 2023), and impacts on sensitive cave fauna such as bats (Blehert et al., 2011). Natural caves are oligotrophic and maintain a relatively consistent temperature throughout the year (Barton and Jurado, 2007; Barton et al., 2007). Show caves disrupt this natural equilibrium by the installation of artificial lighting, stairs, and trails and by inputs from human visitors (Saiz-Jimenez, 2012; Cigna, 2019; Biagioli et al., 2023). In addition, microplastic deposition is considered a biomarker for anthropogenic impact and has also been documented in cave sediments and karst aquifers (for example, see summary papers by Balestra et al., 2023; Hasenmueller et al., 2023; Piccardo and Bevilacqua, 2024), and similar observations have also been documented in southern Appalachian caves (Riley, 2024). These human-induced alterations can contribute to changes in cave microbial biodiversity (Fernandez-Cortes et al., 2011; Gillieson, 2011; Biagioli et al., 2023).

Many caves contain dark brown to black manganese (Mn) oxide biofilms or ferromanganese deposits comprised of higher concentrations of Mn and Fe than the surrounding bedrock (Northup et al., 2003; Carmichael and Bräuer, 2015). Field evidence from epigenic caves in the southern Appalachian Mountains indicates that Mn oxidation is stimulated by

[1]Department of Geological and Environmental Sciences, Appalachian State University, Boone, NC
[2]Department of Geography, McGill University, Montreal, Québec H3A 0G4
[3]Department of Biology, Appalachian State University, Boone, NC, 28608
[4]Stallergenes Greer, Lenoir, NC, 28645
[C]Corresponding author: carmichaelsk@appstate.edu.

exogenous carbon input into carbon-limited environments (Carmichael et al., 2013a, 2013b, 2015; Cloutier et al., 2017), which may vary spatially and temporally (He et al., 2024) and may also be influenced by epikarst (Pipan and Culver, 2013). We hypothesize that cave bedrock mineralogy and geochemistry may strongly influence these processes as well. Indeed, the impact of mineral type (Hutchens et al., 2010) or host rock (Barton et al., 2007) on microbial communities and the interactions of specific microorganisms with specific minerals (Kosznik-Kwaśnicka et al., 2022) have been well documented. In this study, we sought to determine to what degree (if any) human visitation and modification of the cave environment may influence cave mineralogy and/or geochemistry as well as microbial community assemblages. If this relationship appears robust, we can then characterize microbial assemblages in cave sediment as potential biomarkers that can represent different types of human impact.

SITE DESCRIPTIONS

Three caves from the Southern Appalachian Mountains were sampled for this study (Fig. 1, Table 1). We compared a developed show cave (Linville Caverns) with two wild caves: one that hosts tour groups as well as recreational cavers (Worley's Cave) and one that is gated, locked, and closed to the public (Daniel Boone Caverns).

Linville Caverns (LC) is located in McDowell County, North Carolina, along the North Fork of the Catawba River. It is in the Eastern Blue Ridge tectonic province and is hosted in the Cambrian Shady Dolomite, within a structural karst window between the Chattahoochee–Holland Mountain Fault and Cambrian siliciclastic rocks of the Grandfather Mountain Window (Thigpen et al., 2022). The cave is surrounded by hardwood and rhododendron forest (surrounded by the Pisgah National Forest) and is located in extremely steep terrain. It is a highly trafficked show cave that has been active since 1937 (https://www.linvillecaverns.com), receiving over 100,000 visitors a year (official Linville Caverns tourism brochure). A concrete path covers most of the floor in areas open to the public, and stairs, handrails, and artificial lights are present in certain areas as well.

Worley's Cave is found within the Ordovician Knox Dolomite of the Western Valley and Ridge province in Sullivan County, TN (near Bluff City, TN). It is structurally associated with the footwall of the Holston-Iron Mountain thrust sheet (Hatcher et al., 2007) and is surrounded by a mix of single family homes, small hardwood forest tracts (approximately 1–2 acres), and small agricultural fields raising both cattle and hay. It is frequently visited by recreational cavers and adventure tourism groups (estimated by the authors at ~10,000 visitors per year, as no publicly available records are kept). The cave contains a subterranean creek and is hydrologically linked to sinkholes in neighboring farm fields (Burnham et al., 2016).

Daniel Boone Caverns in Scott County, Virginia, is rarely visited and can therefore be considered a pristine cave (Carmichael et al., 2013a, 2015). It is located in the Eastern Valley and Ridge tectonic province, approximately 64 km northeast of Worley's Cave, and is also hosted within the Ordovician Knox Dolomite. It is located on the St. Paul-Honaker thrust sheet (Kulander and Dean, 1986) between the Copper Creek and Clinchport thrust faults (Virginia Division of Mineral Resources, 1993). It contains several drip pools, but lacks a complex subsurface hydrologic system; its location on an isolated ridge within a hardwood forest indicates that it does not experience any agricultural or municipal runoff, which has been confirmed with water testing (Carmichael et al., 2013a, 2013b).

MATERIALS AND METHODS

Sampling Protocol

Sites within each cave were chosen to assess the variability in microbial structures based on the amount of human foot traffic, manganese oxidation, and/or artificial light exposure (Table 2). All samples were taken from horizontal surfaces such as terraces, shelves, and the cave floor, rather than from vertical cave walls. Samples were taken by scraping the collection tube along the sample site's surface and placed on ice to be transported back to the lab. Samples were stored at −80 °C, with splits taken for whole-rock geochemical and mineralogical analysis. Manganese oxidation was detected using the Leucobeurbelin blue (LBB) assay (Krumbein and Altmann, 1973). In addition to the 21 samples taken from inside the cave, two surface samples of representative sediment/soil were taken in Falcon tubes from outside of the entrance of each cave: each cave had sediment sampled from the pathway directly in front of the cave entrance, and associated soil/sediment was taken at least 2 m from the cave entrance. Additional reference soil and sediment samples were taken from locations >2 m from each cave entrance where visitors do not walk, and were used as comparisons with cave sediment that may have experienced human foot traffic. These samples were analyzed with scanning transmission electron microscopy (see Geochemistry and Mineralogy, below), to determine if cave sediment mineralogy and any distinctive nanoparticles were influenced by human traffic coming into the cave or were naturally occuring in the soil.

Foot traffic levels were categorized as *High, Medium, Low*, and *Very Low*. These categories were qualitatively assigned based on direct observations of where tour groups go within show caves, as well as communications with cave owners about the number of visitors per year. The estimated number of visitors is summarized in Table 1. *High* traffic indicates an area with significant, repeated foot traffic, such as main footpaths along guided tour areas. *Medium* traffic

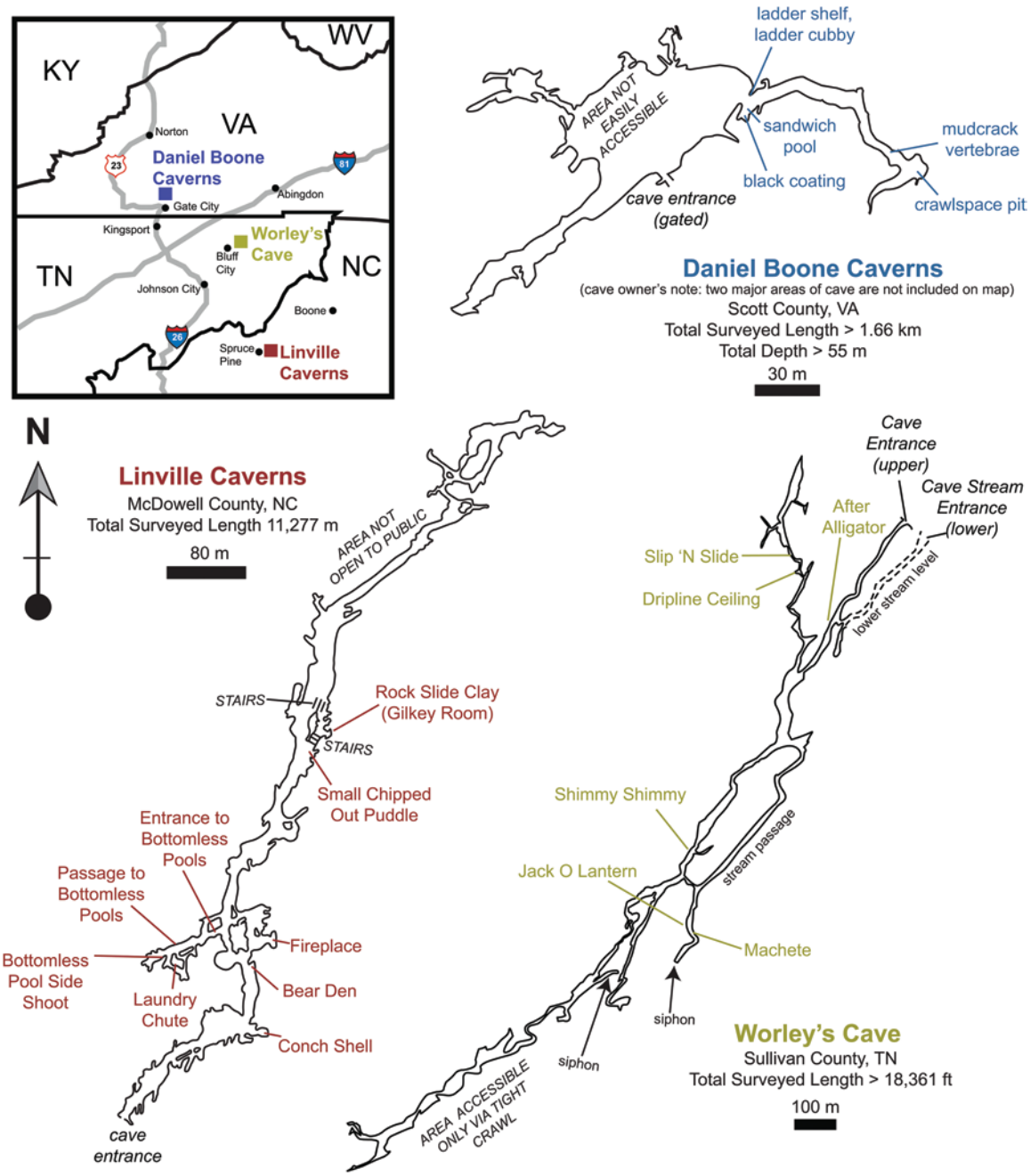


Figure 1. Maps of Linville Caverns, Daniel Boone Caverns, and Worley's Cave with the entrances and sample sites marked. Sample locations are shown using the corresponding color to the cave label and are described in detail in Table 1. Inset shows the relative locations of the three caves within NC, TN, and VA. Linville Caverns map modified from Bailey et al. (1987), and Worley's Cave and Daniel Boone Caverns maps modified from Carmichael et al. (2013a) and Cloutier et al. (2017).

indicates areas where it is easily possible to go off the main path, but tours do not typically bring visitors through the area. *Low* traffic indicates areas where the public is not necessarily prohibited from going but would be unlikely to go to on their own. *Very Low* traffic areas are places where the public is not permitted to go.

Twenty-one sediment samples were collected across the three caves. Linville Caverns had nine sample sites within the cave, representing varying levels of foot traffic, artificial lighting, and manganese oxidation. Six samples were taken from Worley's Cave: three from sites with little to no Mn oxidation, and three from sites that showed signs of current Mn oxidation (of these, three sites were classified as High foot traffic, while three were classified as Low foot traffic). Six samples were taken from Daniel Boone Caverns as well: three sites with little to no Mn oxidation and three sites with Mn oxidation. All samples from Daniel Boone Caverns were classified as Very Low traffic.

Table 1. Cave descriptions, bedrock geology, and surrounding features.

	Linville Caverns (LC)	Worley's Cave (WC)	Daniel Boone Caverns (DBC)
Bedrock Geology	Shady Dolomite (Cambrian)	Knox Group—Dolomite (Ordovician)	Knox Group—Dolomite (Ordovician)
Appalachian physiographic province	Eastern Blue Ridge	Eastern Valley and Ridge	Western Valley and Ridge
Associated structural features	Chattahoochee–Holland Mountain Fault (karst window), adjacent to Grandfather Mountain Window	Holston-Iron Mountain thrust sheet (footwall)	Between Copper Creek and Clinchport thrust faults
Surface environment	Hardwood and rhododendron forest, surrounded by Pisgah National Forest, on North Fork of Catawba River	Single family housing, subsistence agriculture (cattle, hay), pockets of hardwood forest	Hardwood forest, side of ridge on undeveloped land
Human visitation characteristics	Developed show cave (100,000 visitors/year) with walkways and artificial lighting	Undeveloped show cave, numerous tour groups, and recreational cavers (visitors/year estimated at ~5,000–10,000)	Undeveloped private cave, gated and locked (visitors/year estimated at ~10, including the authors of this paper)

Geochemistry and Mineralogy

Whole-rock geochemistry of cave sediment was performed at Activation Laboratories in Ancaster, Ontario, Canada, using the Lithogeochemistry and Whole Rock Analysis 4E - Exploration package. Mineralogy of cave sediment was assessed using a Shimadzu 6000 powder X-ray diffraction system with a Cu X-ray source, measured from 5°–80° 2θ in the Department of Geological and Environmental Sciences, Appalachian State University. Preliminary mineral identification was assigned via Match! Phase identification software from Crystal Impact, using the American Mineralogist database. Mineralogy was confirmed via scanning transmission and spot transmission electron microscopy with energy dispersive X-ray spectroscopy (STEM, TEM–EDS) at 120 kV and 65.5 µA using a JEOL JEM-1400 TEM with an Oxford Xplore TEM 80 mm^2 EDS detector in the Dewel Microscopy Facility at Appalachian State University.

Microbiology

DNA was extracted using the MP Biomedicals FastDNA spin kit for soil. Sequencing was performed at MR DNA on a MiSeq using the 515/806 primers of the V4 variable region of the 16S rRNA gene. MR DNA (Shallowater, TX, USA) was used for library preparation and sequencing. Forward and reverse sequences were then aligned using DADA2, and the nucleotide lengths were trimmed to <200 and 190 for forward and reverse reads, respectively (Callahan et al., 2016). A minimum overlap of 12 base pairs was established, sequences were denoised, and chimeras were removed. The SILVA 138 SSU database was used to assign taxonomy (McLaren and Callahan, 2021). Sequence data were converted to relative abundances of taxa per group as a proportion of all sequences for use in taxonomic figures (McMurdie and Holmes, 2013). Sequence data were deposited in the NCBI Sequence Read Archive (SRA) under BioProject accession PRJNA1468723.

Statistical Methods and Multivariate Analysis

All statistical analyses were conducted in RStudio (version 2024.04.1+748) (Allaire, 2012). Alpha diversity metrics, including Shannon and Simpson diversities as well as Pielou's evenness (Heip, 1974) and observed richness (Phylum classification), were calculated using the vegan package 2.7-3 (Oksanen et al., 2007) in RStudio. Pielou's evenness was calculated using Shannon diversity divided by the natural logarithm of observed richness. Differences in alpha diversity between caves were assessed using Kruskal–Wallis tests. Beta diversity was determined using Bray–Curtis dissimilarity calculated from phylum-level relative abundance. Two-sample, two-tailed, unpaired *t*-tests were also used to determine any statistically significant differences between the geochemical factors within Mn-positive and Mn-negative samples taken from a cave. Non-metric multidimensional scaling (NMDS) ordinations were made using the metaMDS function in the vegan package 2.7.3 (Oksanen et al., 2007). Ordination stress values were used to assess goodness-of-fit. Community analyses utilized the vegan package 2.7-3 (Oksanen et al., 2007). Figures were generated using the ggplot2 package 4.0.2 (Wickham, 2011). Differences in phylum-level microbial community structure between cave locations, as well as traffic intensities, were assessed using permutational multivariate analysis of variance (PERMANOVA) with the adonis2 function (vegan package 2.7.3) using 9999 permutations. Single- and marginal-effect models were assessed with independent effects of cave location and human traffic intensity on microbial community composition. Relationships between microbial communities and geochemical variables were evaluated using environmental fitting (envfit) and overlayed onto NMDS ordinations to determine variables associated with community clustering. Ordination ellipses were plotted at the 99% confidence level grouped by cave location.

Table 2. Sample site descriptions denoting the presence (+) or absence (−) of Mn oxidation, the amount of human traffic in the area, the presence of artificial lighting, and dominant mineralogy. Mineralogy assessed via powder X-ray diffraction (XRD) and/or transmission electron microscopy with energy dispersive X-ray spectroscopy (TEM–EDS) when needed. Some trace mineral structures were not identifiable via TEM–EDS, so are noted only by mineral formula or metal oxide group.

Sample Site	Cave	Mn +/−	Traffic	Light Level	Visual Site Description	Mineralogy
After Alligator	WC	(+)	High	No light	Approximately 1 m after alligator graffiti on way into cave	Quartz$^{(m)}$, illite, microcline, chlorite$^{(tr)}$
Machete	WC	(+)	Low	No light	Gravel stream bank at bend in stream passage; machete had been stabbed into the gravel at the time of sampling.	Quartz$^{(m)}$, illite, chlorite, microcline, birnessite$^{(tr)}$
Jack O Lantern	WC	(+)	Low	No light	Large flowstone deposit in stream passage; sample taken from clay and gravel underneath flowstone.	Quartz$^{(m)}$, illite$^{(tr)}$, chlorite$^{(tr)}$, microcline$^{(tr)}$
Shimmy Shimmy	WC	(−)	High	No light	Steep drop in cave before stream access; requiring “shimmying” down on all fours to the grab sample	Quartz$^{(m)}$, illite, chlorite, microcline
Dripline Ceiling	WC	(−)	Low	No light	Linear series of small (5 cm diameter) drip pools in clay floor from ceiling cave bacon drips above; forming line of puddles full of pebbles	Quartz$^{(m)}$, illite, chlorite, microcline
Slip ‘N Slide’	WC	(−)	High	No light	Clay bank with slippery ramp that leads down into Dripline Ceiling	Quartz$^{(m)}$, illite, chlorite, microcline
Ladder Shelf	DBC	(+)	Very low	No light	Small clay shelf near first ladder leading down into pit	Microcline$^{(m)}$, quartz, illite
Ladder Cubby	DBC	(+)	Very low	No light	Small clay hollowed out “cubby” above second ladder	Quartz$^{(m)}$, microcline, illite
Black Coating	DBC	(+)	Very low	No light	Pit below first ladder with lots of black coatings surrounding calcite veins; samples look like ice cream sandwiches	Dolomite$^{(m)}$, quartz, microcline$^{(tr)}$, birnessite$^{(tr)}$
Crawlspace Pit	DBC	(−)	Very low	No light	Small (1 m deep) breakdown pit at the back of the cave, past the mudcrack tunnel when the room opens up	Dolomite, quartz, microcline, calcite, chlorite
Sandwich Pool	DBC	(−)	Very low	No light	Drip pool at base of first ladder	Quartz, microcline, illite, dolomite$^{(tr)}$, chlorite$^{(tr)}$
Mudcrack Vertebrae	DBC	(−)	Very low	No light	Concretion (~20 cm diameter) that looks like large vertebrae, in mudcrack tunnel after cave popcorn crawl	Quartz, microcline
Rock Slide Clay (Gilkey Room)	LC	(+)	Medium	No lights	Small rubble/clay slump in “Gilkey Room” (as named by cave owners)	Illite, quartz, microcline, Fe oxides (biological?), Mn oxides (biological), apatite$^{(tr)}$, TiO_2 nanoparticles in illite clay$^{(tr)}$
Laundry Chute	LC	(+)	Low	No lights	Pit 30 cm in diameter opens into Bottomless Pool, has smooth walls, and looks like laundry chute	Illite$^{(m)}$, microcline, Fe oxides (biological?), TiO_2 nanoparticles in illite clay$^{(tr)}$
Conch Shell	LC	(+)	High	Direct light	Speleothem that looks like conch shell (as named by cave owners)	Illite$^{(m)}$, Mn oxide (biological), detrital rutile$^{(tr)}$, TiO_2 nanoparticles in illite clay$^{(tr)}$
Bottomless Pool Side Shoot	LC	(+)	Low	No lights	Narrow side passage at back of the Bottomless Pool area	Illite, microcline, quartz, dolomite, albite, calcite, Fe oxide$^{(tr)}$, detrital rutile$^{(tr)}$
Passage to Bottomless Pool	LC	(−)	Low	No lights	Main passage to the Bottomless Pool area (passage no longer used by public)	Illite, dolomite, quartz, microcline, albite, calcite, Fe oxide (biological?), TiO_2 nanoparticles in illite clay$^{(tr)}$
Bear Den	LC	(+)	Low	No lights	Hollow at the base of cave wall (as named by cave owners)	*Insufficient sample volume for analysis*
Entrance to Bottomless Pool	LC	(−)	Medium	Lights in proximity	Waiting area near Bottomless Pool, where guides turn off lights	*Insufficient sample volume for analysis*

Continued

Table 2. *Continued*

Fireplace	LC	(−)	High	Direct light	"Fireplace" hollow in cave wall, used as fireplace in 1800s during Civil War (as named by cave owners)	Illite$^{(m)}$, albite, calcite, microcline, TiO_2 nanoparticles in clay$^{(tr)}$
Small Chipped Out Puddle	LC	(−)	High	Indirect light	Puddle in concrete at base of stairs coming from Gilkey Room; high foot traffic has caused erosion in concrete.	Illite, microcline, calcite, quartz, dolomite, TiO_2 nanoparticles in clay$^{(tr)}$, iron oxide (appears biological)$^{(tr)}$

WC—Worley's Cave; DBC—Daniel Boone Caverns; LC—Linville Caverns.
^{m} = major component (dominant) and ^{tr} = trace component.

Principal component analyses were performed with the software PAST v. 1.81 (Hammer et al., 2001). Raw microbiology data were assessed using cluster analysis with a Bray–Curtis similarity index (Bray and Curtis, 1957), which remains a widely used coefficient in microbial ecology. Both microbiology data (phylum and class) and whole-rock geochemical data were analyzed separately using Principal Component Analysis (PCA), as PCA is the best way to visualize microbial abundance data across relatively similar sites (Ramette, 2007).

Prior to PCA, microbial data were first normalized using an arcsine transform function (commonly used for normalizing microbial abundance data). For PCA and cluster analysis of microbial communities, only the top 20 most abundant phyla and classes are included here for simplicity and image clarity, as the PCA results were nearly identical to those obtained when the entire data sets were used and therefore did not change the hypotheses outlined in the paper. The percentage of variance explained by each principal component is summarized in Table 3. PCA scores and PC loadings are provided in the Supplemental Files for the top 20 phyla/classes, as well as the entire data set.

PCA on whole-rock geochemical data was pre-processed via *Z*-score normalization to prevent the major element data from overwhelming important trace element data (and therefore masking important patterns in metal oxidation). For PCA of whole-rock geochemistry, all elemental data were used, and values that were below the detection limit were assigned a random number between zero and the detection limit.

RESULTS AND DISCUSSION

Microbiology

Phylum-level relative abundance demonstrated higher concentrations of Bacteroidota and Pseudomonadota in Linville Caverns and lower concentrations of Crenarchaeota and Methylmirabilota, whereas Daniel Boone Caverns was enriched in Thermoplasmatota, Chloroflexi, and Nitrospirota (Fig. 2). The Conch Shell site in Linville Caverns also revealed a noticeable enrichment in Cyanobacteriota, which is associated with artificial lighting. Similar trends were seen in the class abundance data (Fig. 3), where Linville Caverns had noticeably higher concentrations of Alphaproteobacteria and Bacteroidia, with lower concentrations of Methylomirabilia compared to both Worley's Cave and Daniel Boone Caverns. Both Shannon and Simpson alpha diversity indices (Fig. 4) indicate overall moderate alpha diversity across samples with high variability between samples, particularly in Linville Caverns. However, there were no obvious differences between caves for either index. Pielou's evenness and observed richness also show relatively similar patterns (Fig. 4). Kruskal–Wallis *p*-values for each metric of phylum-level community structure are all >0.15, indicating that alpha diversity is not particularly significant.

Cluster analysis (Fig. 5) of the top 20 phyla indicates that the major differences in cave microbial community structure appear to be dominated by cave-specific parameters (a combination of bedrock, soils, regional groundwater patterns, etc.), as individual caves tend to cluster together. This analysis shows an outlier group of three sites in Linville Caverns (Rock Slide Clay, Fireplace, and Small Chipped Out Puddle), which all show high to medium human foot traffic; these sites were associated with higher levels of Bacteriodota and Pseudomonadota and lower levels of Methylomirabilota than the other cave sites. Daniel Boone Caverns was particularly depleted in Pseudomonadota compared to Linville Caverns and Worley's Cave (Fig. 5), which likely represents lower anthropogenic impact. This depletion is likely due to lower visitation rates but could possibly also reflect lower amounts of allochthonous carbon from residential septic systems and/or from cattle. However, Linville Caverns has no nearby residential septic systems or cattle; so, this depletion is likely due to human visitation rather than non-point-source environmental carbon sources.

PCA of the top 20 phyla (Fig. 6) and classes (Fig. 7) more efficiently visualizes the patterns across the three cave sites and indicates that many of the cave sites reflect a combination of human traffic and cave-specific microbiomes, regardless of the amount of light or Mn oxidation. Table 3 summarizes the microbes most responsible for the variability across the sample sites, based on the PC loadings representing 95% of the variability within the microbial communities across all 21 sites (see Supplemental Tables S4 for phyla PC loadings and S5 for class loadings).

In both phyla and class data, PC1 (~51% of variance) and PC3 (~9% of variance) reflected microbes that are associated with the presence (or absence) of human traffic. Low-traffic samples were enriched in Thermoplasmatota,

Table 3. Principal component percent variance for the top 20 most abundant phyla and classes for all samples. Each principal component (PC) represents which organisms are primarily responsible for the variance across samples (loadings). When cumulative percent variance reached 95%, the loadings for additional principal components were not assessed as their contribution was negligible. Figures 5 and 6 show additional details for microbial communities for each PC.

Principal Component (PC)	Phylum % Variance (Cumulative)	Phyla Responsible for Variance	Class % Variance (Cumulative)	Classes Responsible for Variance
1	50.9 (50.9)	Bacteroidota, Pseudomonadota, Thermoproteota, Methylmirabilota	51.35 (51.35)	Bacteroidia, Alphaproteobacteria, Nitrososphaeria, Methylmirabilia
2	12.1 (63)	Methylmirabilota, Thermoplasmatota, Acidobacteriota, Cyanobacteriota	10.24 (61.59)	Methylomirabilia, Anaerolineae, Nitrospiria
3	9.5 (72.5)	Chloroflexota, Thermoproteota, Nitrospirota, Thermoplasmatota	9.1 (70.69)	Thermoplasmata, Anaerolineae, Nitrospiria, Alphaproteobacteria, Cyanophyceae
4	7.8 (80.3)	Methylmirabilota, Thermoproteota, Acidobacteriota	7.64 (78.32)	Nitrososphaeria, Vicinamibacteria
5	5.5 (85.8)	Cyanobacteria	7.26 (85.58)	Gammaproteobacteria, Blastocatellia, Thermoanaerobaculia, Thermoplasmata, Cyanophyceae
6	3.9 (89.7)	Verrucomicrobia, Cyanobacteriota, Chloroflexi, Actinomycetota	4.75 (90.33)	Cyanophyceae
7	2.5 (92.2)	Nitrospirota, Bacillota	2.13 (92.46)	Verrucomicrobiia, Polyangia, Blastocatellia
8	2.2 (94.5)	Acidobacteriota, Planctomycetota	2.05 (94.5)	Blastocatellia, Phycisphaerae, Vicinamibacteria
9	1.6 (96.1)	*Not assessed*	1.58 (96.08)	*Not assessed*
10	1.2 (97.3)	*Not assessed*	0.99 (97.07)	*Not assessed*
11	0.8 (98.1)	*Not assessed*	0.79 (97.86)	*Not assessed*
12	0.7 (98.8)	*Not assessed*	0.72 (98.58)	*Not assessed*
13	0.5 (99.3)	*Not assessed*	0.51 (99.1)	*Not assessed*
14	0.3 (99.6)	*Not assessed*	0.36 (99.46)	*Not assessed*
15	0.2 (99.8)	*Not assessed*	0.25 (99.71)	*Not assessed*
16	0.1 (99.9)	*Not assessed*	0.16 (99.87)	*Not assessed*
17	0 (100)	*Not assessed*	0.08 (99.95)	*Not assessed*
18	0 (100)	*Not assessed*	0.02 (99.98)	*Not assessed*
19	0 (100)	*Not assessed*	0.02 (100)	*Not assessed*
20	0 (100)	*Not assessed*	0 (100)	*Not assessed*

Chloroflexota, and Nitrospirota along PC3 and Thermoproteota and Methylomirabilota along PC1 (Fig. 6). Interestingly, along PC1, high-traffic samples were enriched in Bacteroidota and Pseudomonadota, two of the four human-associated phyla. Along PC2 (10%–12% of variance), the clustering pattern simply reflects cave-specific microbiomes where each cave clusters together, and the microbes responsible for the variability in PC2 are all cave/soil microbes typical of this region, as shown in Lange-Enyedi et al. (2023), Turrini et al. (2024), and Martin-Pozas et al. (2025). These are also microbes associated with clays (Chen et al., 2018) (see Table 2 for specific minerals associated with each site). None of the variance in the top 20 phyla shows any robust relationships between light levels or Mn oxidation, with the exception of Cyanobacteriota, which is next to an artificial light source in Linville Caverns.

Not surprisingly, PCA patterns for microbial class data are similar to those of the phyla data (Fig. 7); PC1 shows enrichment in Bacteroidia and Alphaproteobacteria in medium/high-traffic areas, and enrichment in Nitrososphaeria and Methylmirabilia in low-traffic areas (Fig. 6). There is more overlap in PC3 between high-traffic and low-traffic sites, but some very low-traffic areas show enrichment in Thermoplasmatota, Anaerolineae, and Nitrospiria. Several genera known to oxidize Mn were detected, including *Pseudomonas*, *Leptothrix*, and *Flavobacterium* (Carmichael et al., 2013a) as well as *Pedomicrobium* and *Caulobacter* species (Lozano and Rossi, 2012) and *Pseudoxanthamonus* (Ashassi-Sorkhabi et al., 2012). Since the process of Mn oxidation is polyphyletic and quite complex (Tebo et al., 2005, 2007; Geszvain et al., 2012; Hansel and Learman, 2016; Yu and Leadbetter, 2020), particularly in caves (Carmichael and Bräuer, 2015), it is unclear if these phyla are actually involved in Mn oxidation *in situ*.

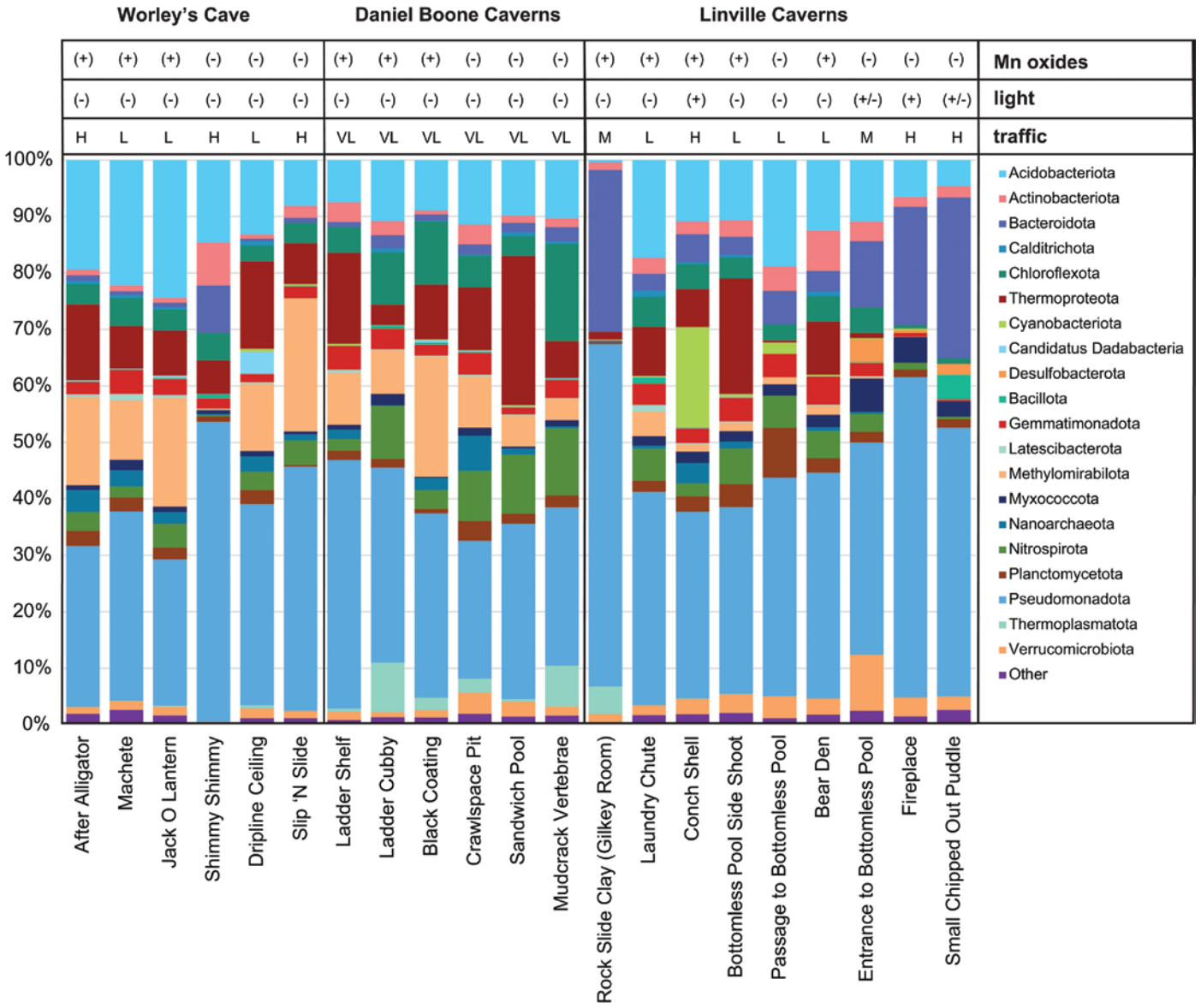


Figure 2. Phylum-level relative abundance of sequence reads across samples collected in all three caves. Manganese oxide notation of (+) indicates a positive LBB test, (−) indicates a negative LBB test. Light levels of (−) indicate no light (aside from caver headlamps or flashlights), (+/−) indicate indirect light, and (+) indicate direct light. Traffic is noted as H (high), M (medium), L (low), or VL (very low), as described in the sampling protocol.

Our microbial results align with previous research, indicating that Bacteroidota (formerly Bacteroidetes) serve as a critical signature of anthropogenic impact in cave environments. Specifically, work by Bontemps et al. (2022, 2023) demonstrates that human activity leads to the deposition of labile organic matter, which promotes a bloom of these bacteria in dark zone stains threatening Paleolithic art. Bacteroidota are characterized as copiotrophic due to their association with carbon amendment and their specialized ability to hydrolyze high-molecular weight organic matter, such as proteins, carbohydrates, and other nutrient-rich substrates (Fierer et al., 2007; Thomas et al., 2011). In particular, these "selfish" bacteria accumulate substrates like laminarin (Brown et al., 2024), while specific clusters like *Cytophaga-Flavobacter* show enrichment with chitin and protein (Cottrell and Kirchman, 2000). Our observations of increased *Chitinophagales*, *Flavobacteriales*, and *Cytophagales* within Linville Caverns sediments support these findings, as do the elevated concentrations of *Flavobacteriaceae* genera—such as *Formosa*, *Polaribacter*, *Ulvibacter*, and *Flavobacterium*—which are known to thrive when labile organic carbon is introduced (von Jackowski et al., 2022). This relationship is mirrored in preliminary microplastics data from all three caves (Riley, 2024), where Linville Caverns had far more microplastic and microfiber particles than Daniel Boone Caverns or Worley's Cave.

Additionally, artificial lighting may influence microbial composition at the Conch Shell site (the only site receiving direct light), where Cyanobacteriota were enriched relative to other sampling locations (Table 2). This was also the

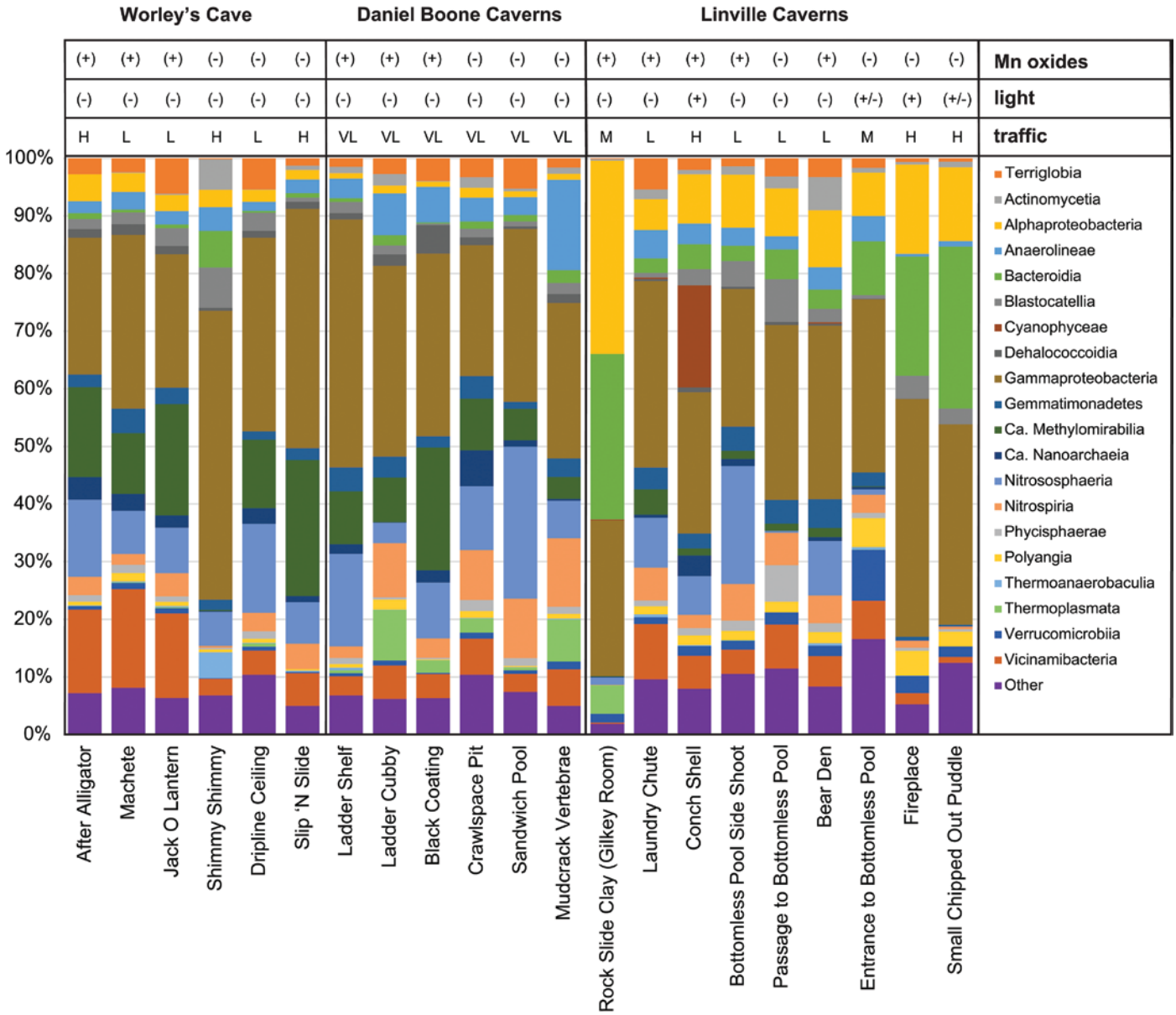


Figure 3. Class-level relative abundance of sequence reads across samples collected in all three caves. Manganese oxide notation of (+) indicates a positive LBB test, (−) indicates a negative LBB test. Light levels of (−) indicate no light (aside from caver headlamps or flashlights), (+/−) indicate indirect light, and (+) indicate direct light. Traffic is noted as H (high), M (medium), L (low), or VL (very low), as described in the sampling protocol.

only sample with a visible green patina present (Riley, 2024). Enrichment of Cyanobacteriota in cave systems via the use of artificial lighting has been documented in previous studies (Lamprinou et al., 2014; Czerwik-Marcinkowska and Massalski, 2018; Burgoyne et al., 2021), while others have noted changes in algal communities in caves due to artificial lighting (Biagioli et al., 2023).

Mineralogy and Geochemistry

X-ray diffraction of bulk sediment was combined with major, trace, and rare earth element (REE) whole-rock geochemistry data to determine the mineralogy of the sediment (Table 2). Mineral identifications were confirmed with transmission electron microscopy with energy-dispersive X-ray spectroscopy (TEM–EDS) analysis of individual sediment particles. Whole-rock geochemical data are provided in Supplemental Tables S1, S2, and S3. The sediments across the sample sites include combinations of fine silt-sized quartz and feldspar (dominantly microcline with minor albite), chlorite and illite clay, sand-sized grains of calcite and dolomite (from physical weathering of the cave walls), trace amounts of Fe oxides and Mn oxides (likely birnessite, which is the most common Mn oxide mineral in caves; see review by Carmichael and Bräuer, 2015) and TiO_2 nanoparticles.

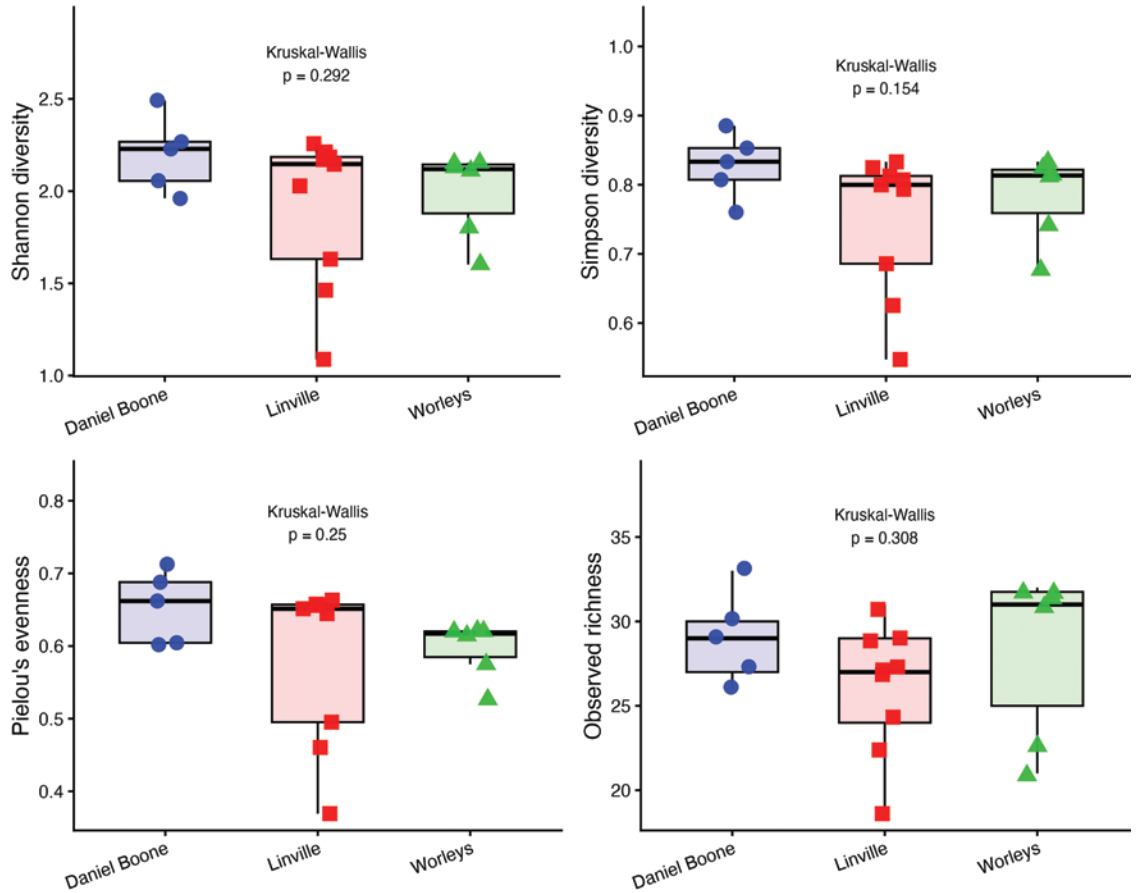


Figure 4. Alpha diversity metrices for phylum-level microbial communities between cave location. Panels show Shannon (top left) and Simpson (top right) diversities, as well as Pielou's evenness (bottom left) and observed richness (bottom right). Kruskal–Wallis *p*-values are shown within each panel.

Despite some clear indicators of anthropogenic sediment supply in TEM analysis of particles in Linville Caverns, anthropogenic particles were volumetrically insignificant compared to clay and silt particles. TiO_2 nanoparticles were present in both illite clay particles and quartz grains (Fig. 8) but did not appear to be introduced by human foot traffic even though these nanoparticles are extremely common in industrial products, sunscreen, shoe soles, etc. Soil samples taken from outside of each cave in areas where people do not walk also showed these nanoparticles in illite and quartz grains, and sediment samples from a carpet outside of the entrance to Linville Caverns did not show any unusual TiO_2 nanoparticle enrichment, so it is likely that these nanoparticles represent original mineral features from the overlying soils or from within the bedrock itself. This is not unexpected, as quartz commonly contains TiO_2 nanoparticles, particularly quartz formed during metamorphism (Ostapenko et al., 2007), and metamorphic quartz is common throughout the Proterozoic Blue Ridge basement rocks as well as the younger Paleozoic Valley and Ridge sediments of the southern Appalachians. Illite commonly contains TiO_2 nanoparticles because its crystal structure retains nanoparticles better than other types of clay minerals (Bayat et al., 2015).

Z-score transformed PCA plots of whole-rock geochemistry (Fig. 9) demonstrated that geochemical variance is mostly determined by host bedrock type combined with localized sample differences. PC1 (36% of variance) simply represents the amount of wall rock in the individual sediment sample (and is therefore not graphed), PC2 (16% of variance) represents the amount of clay minerals vs. detrital feldspars, and PC3 (12% of variance) represents the amount of detrital heavy minerals vs. Mn oxidation and phosphate (as shown in Fig. 8); 36% of the remaining variability is based on geochemical relationships that are less clear (Table 4, with specific loadings shown in Supplemental Table S6). Mn oxidation showed a weak signal in PCA but was still present in PC3 and may have correlation with an organic phosphate source.

Geochemical differences between sites that are Mn+ and Mn− show some correlations according to *t*-tests (Table 5), particularly in Linville Caverns, but PCA combined with TEM-EDS and XRD analysis gives a more coherent picture of the relationship (or lack thereof) between Mn oxidation and geochemistry. PC1, PC2, and PC3 patterns are reflected in the XRD and TEM–EDS analyses, where Linville Caverns has significantly more apatite/phosphate and clay materials

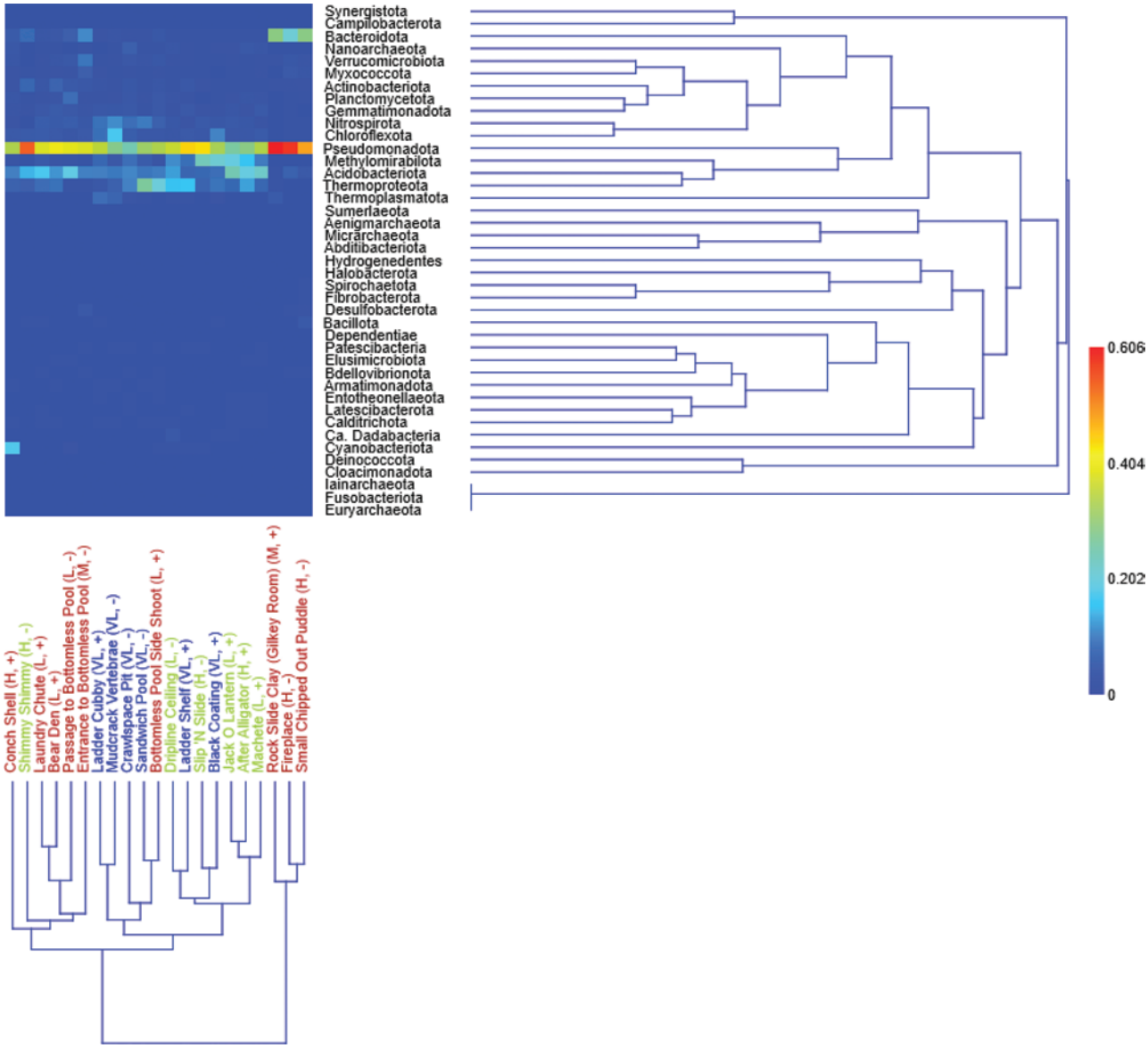


Figure 5. Two-way cluster analysis and heat map of phylum level abundance and cave groups using a Bray Curtis similarity index and raw abundance data. Worley's Cave sample locations are noted in green text, Daniel Boone Caverns in blue text, and Linville Caverns samples in red text. Traffic levels are denoted by H, M, L, and VL (high, medium, low and very low, respectively). Mn oxidation was noted as present or absent (+ or −) through Leucoberbelin Blue assays in the field. Using this similarity index, cave microbial community structure generally seems (with few exceptions) to be dominated by cave parameters (a combination of bedrock, soils, regional groundwater patterns, etc.) with an outlier group in Linville Caverns showing high-medium human foot traffic; these sites were associated with higher levels of Bacteriodota and Pseudomonadota and lower levels of Methylomirabilota than the other cave sites.

in its sediment, while Daniel Boone Caverns and Worley's Cave are enriched in quartz, feldspars, and detrital heavy minerals (Table 2). These clustering patterns likely reflect the original clastic sediments within the Knox Dolomite (hosting Worley's Cave and Daniel Boone Caverns) and the Shady Dolomite (hosting Linville Caverns), and variability within each cave likely only reflects local changes in sediment source at the time these rocks were deposited (see Mussman and Read, 1986; Montañez and Read, 1992; and Smoot and Southworth, 2014 for a more detailed sedimentological history of these rock units).

Non-metric multidimensional scaling (NMDS) combining sediment geochemistry and phylum-level community structure primarily demonstrates clustering according to cave and possibly exposure to traffic (Fig. 10). When combined with phylum data, a correlation of geochemistry with Mn oxidation (either + or −) was not present in NMDS patterns despite the *t*-test associations between Mn oxidation and (as shown in Table 5). When combined with geochemical data, correlation with traffic (recategorized as either H = high, or L = low, for better visualization) was no longer present despite being a driving factor in phylum-level data. The addition of average particle size data to NMDS analysis of geochemistry and

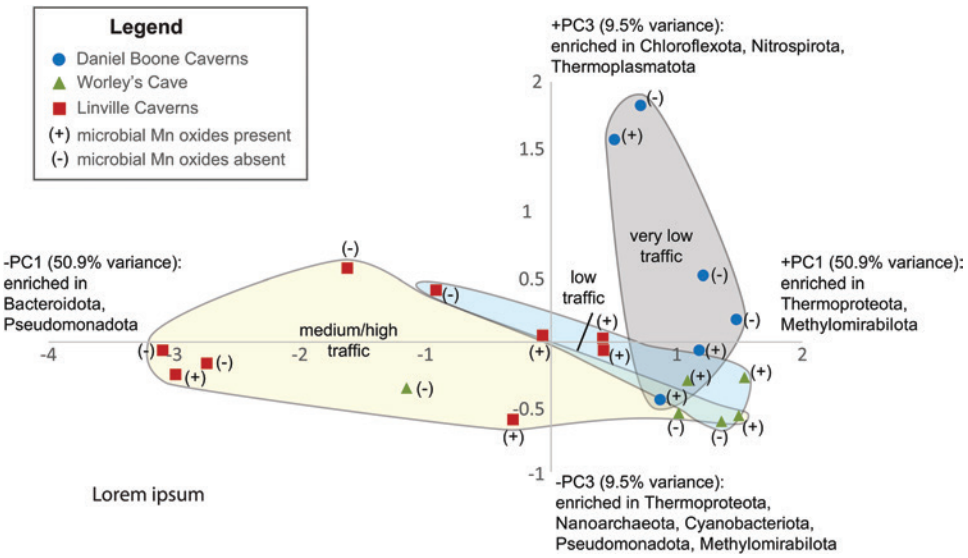


Figure 6. PCA of the top 20 most abundant phyla; samples that are more similar plot closer together, whereas samples that are more different plot farther apart. Samples from Linville Caverns are indicated by red squares, Daniel Boone Caverns by blue circles, and Worley's Cave by green triangles. There is a noticeable lack of overlap between samples classified as "high traffic," "low traffic," and "very low traffic" as defined in Table 2. Samples classified as "high traffic" have less Methylomirobilota and more Proteobacteria and Bacteriodoita than samples classified as "low traffic" and "very low traffic."

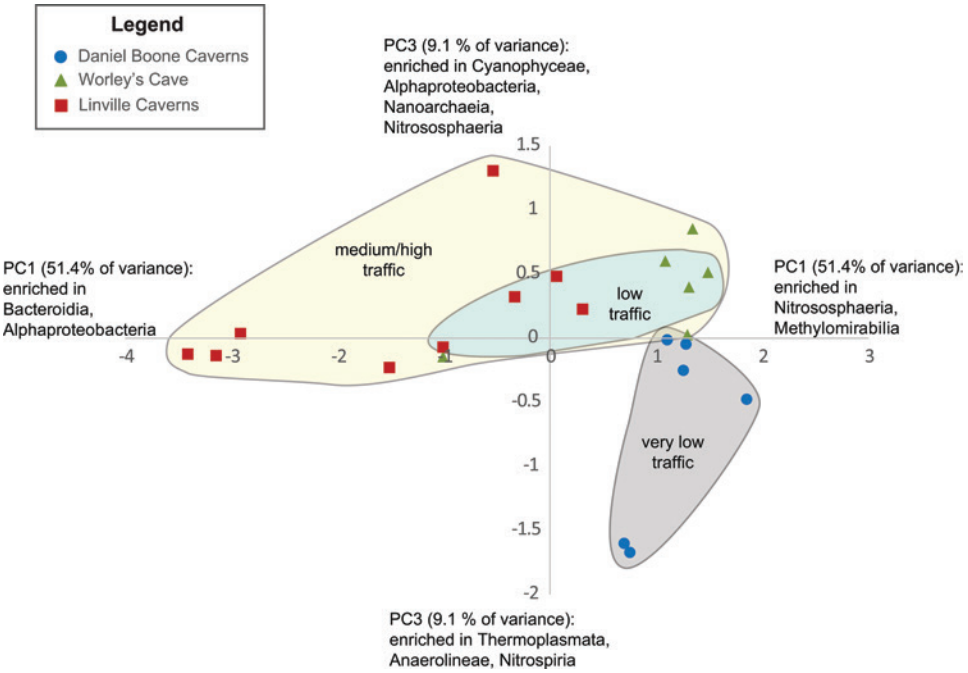


Figure 7. PCA of the top 20 most abundant classes of microbes; samples that are more similar plot closer together, whereas samples that are more different plot farther apart. Samples from Linville Caverns are indicated by red squares, Daniel Boone Caverns by blue circles, and Worley's Cave by green triangles. There is a noticeable lack of overlap between samples classified as "very low traffic" as defined in Table 2 with other traffic levels, and a trend towards enrichment in Cyanobacteriota, Bacteroidia, Alphaproteobacteria, and Nanoarchaeia as traffic levels increase.

phyla data did not change any results (Norvell, 2023), so particle size is unlikely to be a driver of microbial patterns.

PERMANOVA using Bray–Curtis dissimilarities (Table 6) assessed the independent effects of cave location and traffic intensity and showed that human traffic is associated with microbial community composition (also shown in PERDISP analysis). Cave sediment geochemistry also independently influences microbial community structure, per PERMANOVA and envfit testing. In particular, wt% Na_2O and trace elements Sr and Cs also have a strong correlation with community structure (which is also shown in the NMDS plot in Fig. 10). This relationship can be explained by the cave geochemistry, where (1) there is albite (a sodium rich feldspar) in the cave sediment fraction in Linville Caverns, and (2) there is more illite in the clay fraction of Linville Caverns sediment, and strontium preferentially sorbs to illite clays rather than chlorite clays (Fuller et al., 2016). Cesium is more complicated to interpret, because in our data it is coupled with aluminum concentrations (Supplemental Table S6). As aluminum is present in both feldspars and clays, and all of the cave sediments in this study have a mix of feldspars and clays, it is difficult to decouple which particular Al-bearing minerals are associated with Cs.

Geochemistry is clearly driving changes in microbial communities in our caves that span two distinct bedrock formations. When taken together, our results are consistent with previous studies that show how cave mineralogy (Hutchens et al., 2010; Kosznik-Kwaśnicka et al., 2022; Lange-Enyedi et al., 2023) and human visitation (Tomczyk-Żak and Zielenkiewicz, 2016) have been found to impact cave microbial communities, although cave mineralogy (or associated bedrock-related features such as groundwater and soil chemistry) appears to dominate a cave's microbiome

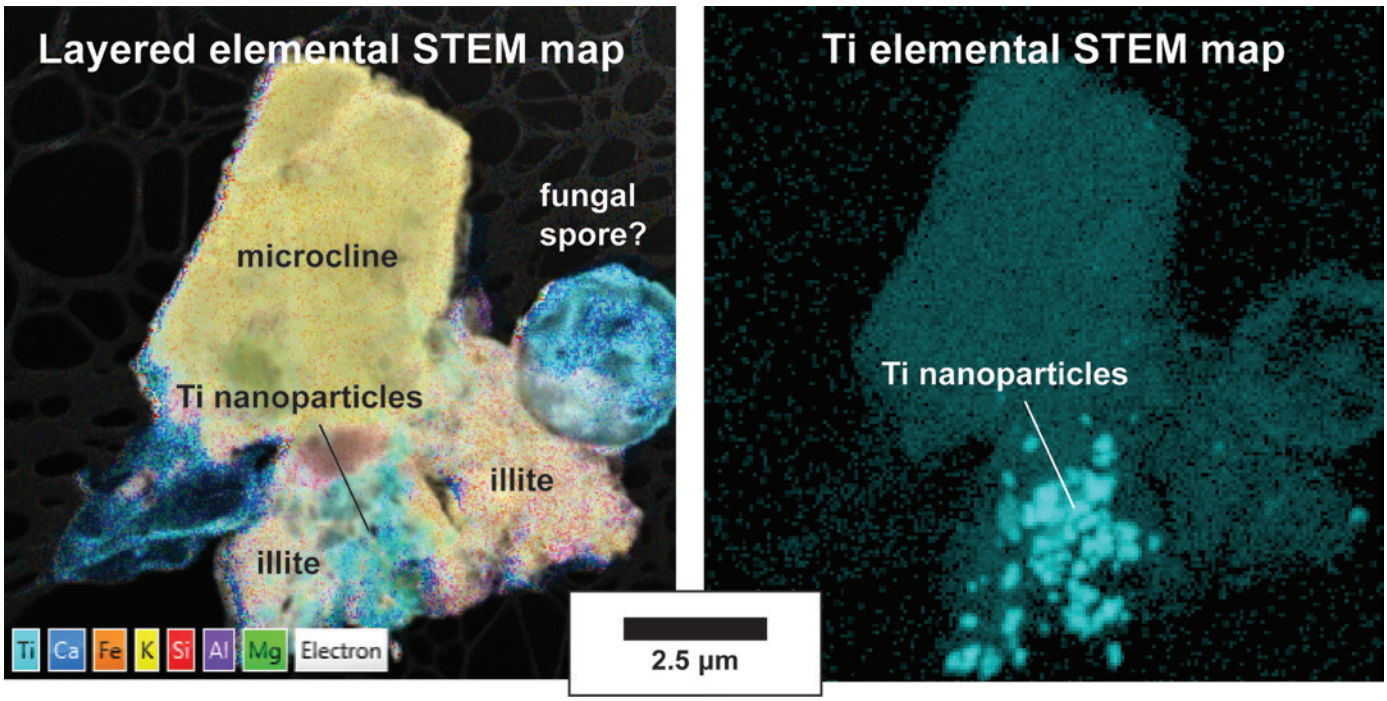


Figure 8. Scanning transmission electron microscopy (STEM) elemental map of sediment from the Rock Slide Clay in the Gilkey Room in Linville Caverns: layered elemental map is on the left, and Ti content is on the left. The round shape to the right of the image is likely a fungal spore. The area containing numerous Ti nanoparticles is a collection of illite clay grains. The larger, yellow grain is a fine silt-sized piece of microcline.

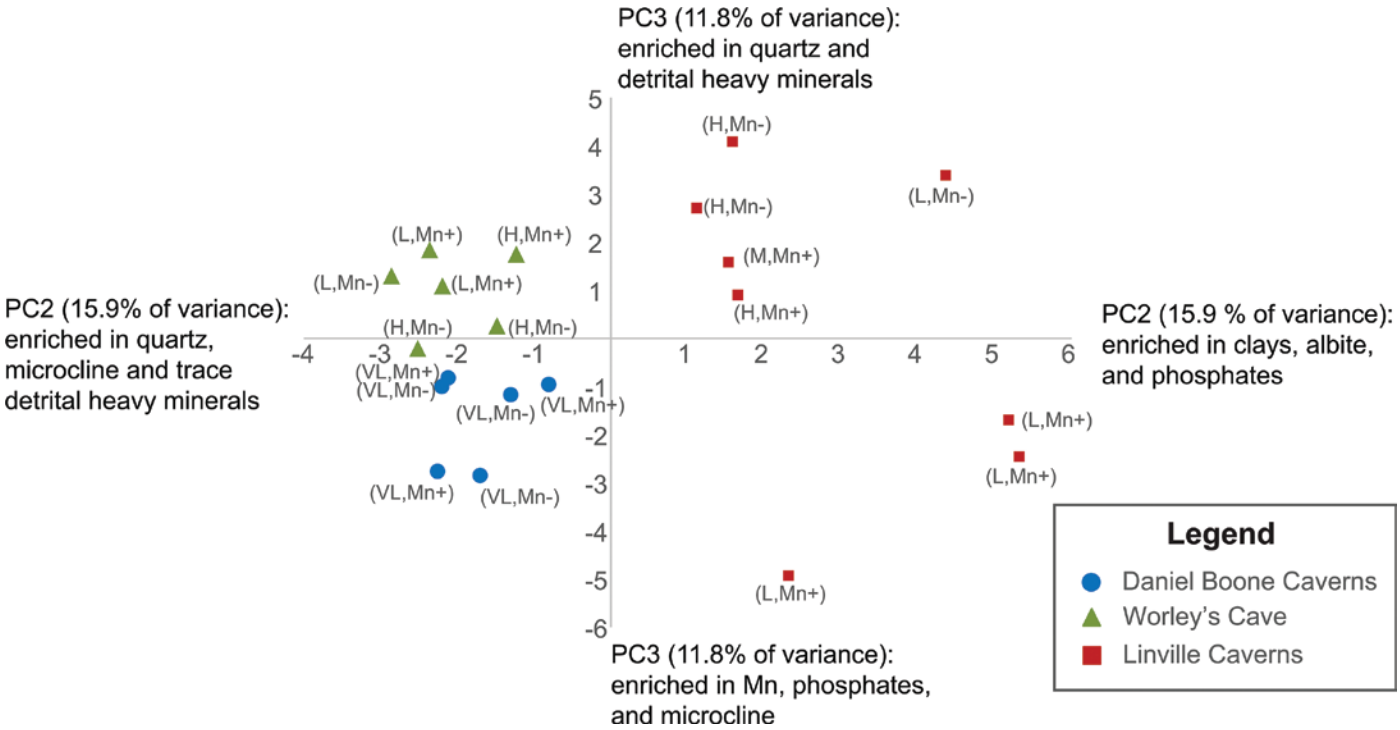


Figure 9. Z-score transformed PCA plots of whole-rock geochemistry of cave sediments using principal components 2 (PC2) and 3 (PC3); samples that are more similar plot closer together, whereas samples that are more different plot farther apart. PC1 is not shown, as it simply reflects the amount of calcite or dolomite host rock incorporated into the sediment through physical weathering of cave passages. For the purposes of this plot, whole-rock geochemistry has been translated into mineralogy based on combining geochemistry, XRD, and TEM–EDS analysis. Samples from Linville Caverns are indicated by red squares, Daniel Boone Caverns by blue circles, and Worley's Cave by green triangles. Traffic levels are denoted by H, M, L, and VL (high, medium, low and very low, respectively). The presence or absence of Mn oxidation is noted at Mn+ or Mn−. There is no obvious clustering in any sites aside from their association with the cave in which they are located, indicating that geochemistry is strongly influenced by bedrock geology.

Table 4. PCA loadings of whole-rock geochemical data (most useful principal components noted as *).

Principal Component (PC)	Geochemistry % Variance (Cumulative)	Minerals Likely Responsible for Variance
1	36.1 (36.1)	Calcite, dolomite (amount of wall rock in the sediment sample) relative to siliciclastic minerals
2*	15.9 (52)	Illite, microcline, chlorite, albite (amount and type of clay relative to the amount and type of detrital feldspars)
3*	11.8 (63.7)	Detrital heavy/refractory minerals relative to the presence of trace Mn- and P-bearing minerals (birnessite? apatite or organic phosphate?)
4	8.9 (72.6)	Weathered sulfides relative to detrital zircon?
5	6.5 (79.2)	Weathered sulfides relative to detrital zircon?
6	4.5 (83.6)	Amount of Mn oxidation?
7	3.6 (87.2)	Unknown; element combinations unclear
8	3.3 (90.5)	Unknown; element combinations unclear
9	2.3 (92.8)	*Not assessed—variance too low*
10	1.8 (94.6)	*Not assessed—variance too low*
11	1.7 (96.3)	*Not assessed—variance too low*
12	1.2 (97.5)	*Not assessed—variance too low*
13	0.8 (98.3)	*Not assessed—variance too low*
14	0.6 (98.9)	*Not assessed—variance too low*
15	0.5 (99.4)	*Not assessed—variance too low*
16	0.3 (99.8)	*Not assessed—variance too low*
17	0.1 (99.9)	*Not assessed—variance too low*
18	0.1 (100)	*Not assessed—variance too low*
19	0 (100)	*Not assessed—variance too low*

Table 5. Significant differences in major element geochemistry (elemental weight %) between Mn-positive and Mn-negative sites within each of the three caves; *p*-values for the *t*-tests are displayed.

Cave	Element	Mn+	Mn−	*p*-value
WC	C	0.58 (0.035)	0.12 (0.055)	0.001
LC	Al	1.48 (0.083)	1.19 (0.122)	0.030
LC	K	0.80 (0.039)	0.64 (0.035)	0.007
LC	Ti	0.39 (0.027)	0.32 (0.005)	0.038

Note: Data from Norvell (2023).

more so than human traffic alone (Figs. 6, 7, and 10).

SUMMARY

Cave bedrock type exerts a strong influence on sediment geochemistry (which is expected), but also on a cave's microbial community structure. The caves in this study differ by bedrock type and also by the number of annual visitors. Although it is uncertain to what degree each of these factors may be driving changes in microbial community assemblages, overall, our research shows that human visitors leave an indelible mark on cave sediments, depositing human-associated bacteria. Our data corroborate studies demonstrating that Bacteroidota are positively correlated and Nitrospirota are negatively correlated with anthropogenic input via human traffic, and that bedrock type also exerts a strong influence on sediment geochemistry and associated microbial communities within the sediment.

ACKNOWLEDGMENTS

We gratefully thank the staff at Linville Caverns for allowing sample collection and their direction throughout the various areas within the cave, John Rossi for his expertise in the field and for guiding the field team through Daniel Boone Caverns, and Milton Starnes for allowing us to collect samples from Daniel Boone Caverns. Lucca Scoggins received support from Appalachian State University's Office of Student Research and the Department of Geological and Environmental Sciences. We would like to extend an additional thanks to Lilith Hazzard for assisting with initial mineral

Table 6. Multivariate statistical analyses showing the relationships between cave location, human traffic, geochemical variables with respect to phylum-level microbial community clustering. PERMANOVA was based on Bray–Curtis dissimilarities, while marginal PERMANOVA models assessed the independent effects of cave location and traffic intensity (high or low traffic). Environmental fitting (envfit) identified geochemical drivers that were significantly related to microbial ordinations.

Test	Factor/ Variable	R^2	*F*	*p*-value	Interpretation
PERMANOVA	Traffic only	0.240	5.67	0.0025	Traffic associated with community composition
PERMANOVA	Cave (marginal)	0.245	3.81	0.0048	Cave identity independently structures communities
PERMANOVA	Traffic (marginal)	0.159	4.94	0.0054	Traffic independently influences community structure
PERMDISP	Traffic	—	8.52	0.0120	Traffic groups differ in multivariate dispersion
envfit	Na_2O	0.579	—	0.0013	Correlated with microbial community structure and feldspar type in cave sediment
envfit	Sr	0.620	—	<0.001	Strong association with NMDS structure, also correlated with clay type in cave sediment
envfit	Cs	0.339	—	0.0366	Opposes Sr/Na_2O environmental gradient

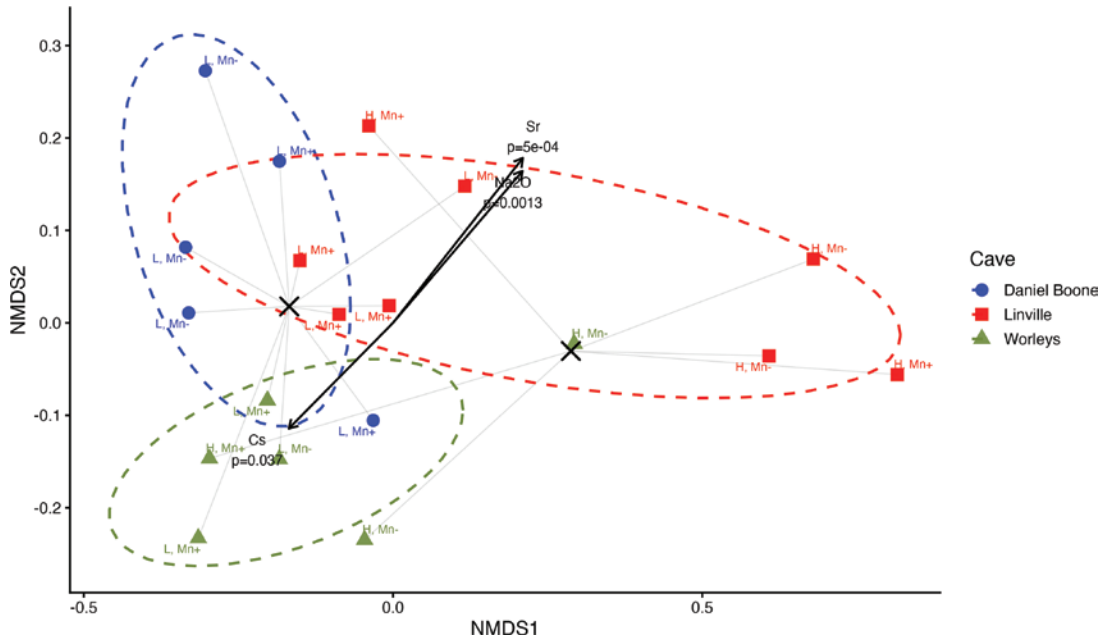


Figure 10. Non-metric multidimensional scaling (NMDS) ordination of phylum-level microbial community structure with only significant geochemical variables (black arrows) using environmental fitting (envfit) with accompanied *p*-values. Dashed ellipses show 99% confidence intervals associated with cave location. Point labels indicate human traffic intensity (H: high traffic, L: low traffic), as well as manganese oxidation status (+ or −). Stress = 0.094.

identification, and Steven J. Hageman for assistance with multivariate analyses. Partial support was provided through a Cave Conservancy Foundation grant to Suzanna Brauer, Sarah Carmichael, and Morgan Smith, and a Cave Research Foundation Graduate Research Grant awarded to Morgan Smith. Support was also provided by Appalachian State University.

SUPPLEMENTAL INFORMATION

Supplemental Tables and Figures.pdf
Phylum raw data (.xls)
Class raw data (.xls)

REFERENCES

Allaire, J., 2012, RStudio: integrated development environment for R: The R User Conference, useR!, https://posit.co/download/rstudio-desktop/.

Ashassi-Sorkhabi, H., Moradi-Haghighi, M., and Zarrini, G., 2012, The effect of *Pseudoxanthomonas* sp. as manganese oxidizing bacterium on the corrosion behavior of carbon steel: Materials Science and Engineering: C, v. 32, no. 2, p. 303–309.

Bailey, J., Adams, L., Adams, K., Holler, N., Bailey, S., Bailey, J., Cunningham, C., Shelton, E., Speer, E., Holler, C., Holler, S., and Holler, C., 1987, Map of Linville Caverns: McDowell County, NC, North Carolina Cave Survey.

Balestra, V., Vigna, B., De Costanzo, S., and Bellopede, R., 2023, Preliminary investigations of microplastic pollution in karst systems, from surface watercourses to cave waters: Journal of Contaminant Hydrology, v. 252, p. 104117.

Barton, H. A. and Jurado, V., 2007, What's up down there? Microbial diversity in caves: Microbe, v. 2, no. 3, p. 132–138.

Barton, H. A., Taylor, N. M., Kreate, M. P., Springer, A. C., Oehrle, S. A., and Bertog, J. L., 2007, The impact of host rock geochemistry on bacterial community structure in oligotrophic cave environments: International Journal of Speleology, v. 36, no. 2, p. 93–104.

Bayat, A. E., Junin, R., Mohsin, R., Hokmabadi, M., and Shamshirband, S., 2015, Influence of clay particles on Al_2O_3 and TiO_2 nanoparticles transport and retention through limestone porous media: measurements and mechanisms: Journal of Nanoparticle Research, v. 17, no. 5, p. 1–14.

Biagioli, F., Coleine, C., Piano, E., Nicolosi, G., Poli, A., Prigione, V., Zanellati, A., Varese, C., Isaia, M., and Selbmann, L., 2023, Microbial diversity and proxy species for human impact in Italian karst caves: Scientific Reports, v. 13, no. 1, p. 1–13

Blehert, D. S., Lorch, J. M., Ballmann, A. E., Cryan, P. M., and Meteyer, C. U., 2011, Bat white-nose syndrome in North America: Microbe, v. 6, p. 267–273.

Bontemps, Z., Alonso, L., Pommier, T., Hugoni, M., and Moënne-Loccoz, Y., 2022, Microbial ecology of tourist Paleolithic caves: Science of the Total Environment, v. 816, p. 151492.

Bontemps, Z., Prigent-Combaret, C., Guillmot, A., Hugoni, M., and Moënne-Loccoz, Y., 2023, Dark-zone alterations expand throughout Paleolithic Lascaux Cave despite spatial heterogeneity of the cave microbiome: Environmental Microbiome, v. 18, no. 1, p. 31.

Brannen-Donnelly, K and Engel, A. S., 2015, Bacterial diversity differences along an epigenic cave stream reveal evidence of community dynamics, succession, and stability: Frontiers in Microbiology, v. 6, p. 729.

Bray, J. R. and Curtis, J. T., 1957, An ordination of the upland forest communities of southern Wisconsin: Ecological Monographs, v. 27, no. 4, p. 325–349.

Brown, S., Lloyd, C. C., Giljan, G., Ghobrial, S., Amann, R., and Arnosti, C., 2024, Pulsed inputs of high molecular weight organic matter shift the mechanisms of substrate utilisation in marine bacterial communities: Environmental Microbiology, v. 26, no. 2, p. e16580.
Burgoyne, J., Crepeau, R., Jensen, J., Smith, H., Baker, G., and Leavitt, S. D., 2021, Lampenflora in a show cave in the Great Basin is distinct from communities on naturally lit rock surfaces in nearby wild caves: Microorganisms, v. 9, no. 6, p. 1188.
Burnham, T., Luffman, I., Whitelaw, M., and Gao, Y., Jr., 2016, Assessing structural control on groundwater flow in the Morrell Cave springshed, Sullivan County, Tennessee, in Feinberg, J. M., Gao, Y., and Alexander, E. C., eds., Caves and Karst Across Time: Geological Society of America Special Paper 516: Geological Society of America, p. 151–164, https://doi.org/10.1130/2015.2516(13).
Callahan, B. J., McMurdie, P. J., Rosen, M. J., Han, A. W., Johnson, A. J. A., and Holmes, S. P., 2016, DADA2: High-resolution sample inference from Illumina amplicon data: Nature Methods, v. 13, no. 7, p. 581–583.
Carmichael, M. J., Carmichael, S. K., Santelli, C. M., Strom, A., and Bräuer, S. L., 2013a, Mn(II)-oxidizing bacteria are environmentally relevant members of ferromanganese deposits in caves of the upper Tennessee River Basin: Geomicrobiology Journal, v. 30, no. 9, p. 779–800.
Carmichael, S. K. and Bräuer, S. L., 2015, Microbial diversity and manganese cycling: A review of Mn-oxidizing microbial cave communities, *in* Engel, A. S., ed., Microbial Life of Cave Systems, Vol. 3: Boston, MA, De Gruyter, p. 137–160.
Carmichael, S., Carmichael, M., Strom, A., Johnson, K., Roble, L., Gao, Y., and Brauer, S., 2013b, Sustained anthropogenic impact in Carter Salt Peter Cave, Carter County, Tennessee and the potential effects on Mn cycling: Journal of Cave and Karst Studies, v. 75, no. 3, p. 189–204.
Carmichael, S. K., Zorn, B. T., Santelli, C. M., Roble, L. A., Carmichael, M. J., and Bräuer, S. L., 2015, Nutrient input influences fungal community composition and size and can stimulate manganese (II) oxidation in caves: Environmental Microbiology Reports, v. 7, no. 4, p. 592–605.
Chen, C., Pan, G., Shi, W., Xu, F., Techtmann, S. M., Pfiffner, S. M., and Hazen, T. C., 2018, Clay flocculation effect on microbial community composition in water and sediment: Frontiers in Environmental Science, v. 6, no. 60, p. 1–10.
Cheng, X., Zhao, R., Bodelier, P. L., Song, Y., Yang, K., Tuovinen, O. H., and Wang, H., 2024, Differential response of subterranean microbiome to exogenous organic matter input in a cave ecosystem: Science of the Total Environment, v. 954, p. 176584.
Cigna, A. A., 2019, Show Caves: Encyclopedia of Caves: Elsevier, p. 909–921.
Cloutier, M. L., Carmichael, S. K., Carson, M. A., Madritch, M. D., and Bräuer, S. L., 2017, Carbon quantity and quality drives variation in cave microbial communities and regulates Mn(II) oxidation: Biogeochemistry, v. 134, no. 1–2, p. 77–94.
Cottrell, M. T. and Kirchman, D. L., 2000, Natural assemblages of marine proteobacteria and members of the Cytophaga-Flavobacter cluster consuming low- and high-molecular-weight dissolved organic matter: Applied and Environmental Microbiology, v. 66, no. 4, p. 1692–1697.
Czerwik-Marcinkowska, J and Massalski, A., 2018, Diversity of Cyanobacteria on Limestone Caves: Cyanobacteria: London, IntechOpen, p. 137–164.
Engel, A., 2010, Microbial diversity of cave ecosystems, *in* Barton, L. L., Mandl, M., and Loy, A., eds., *Geomicrobiology: Molecular and Environmental Perspective*: Springer Netherlands, p. 219–238, https://doi.org/10.1007/978-90-481-9204-5_10.
Faimon, J., Troppova, D., Baldik, V., and Novotny, R., 2012, Air circulation and its impact on microclimatic variables in the Cisarska Cave (Moravian Karst, Czech Republic): International Journal of Climatology, v. 32, no. 4, p. 599–623.
Fernandez-Cortes, A., Cuezva, S., Sanchez-Moral, S., Cañaveras, J. C., Porca, E., Jurado, V., Martin-Sanchez, P. M., and Saiz-Jimenez, C., 2011, Detection of human-induced environmental disturbances in a show cave: Environmental Science and Pollution Research, v. 18, no. 6, p. 1037–1045, https://doi.org/10.1007/s11356-011-0513-5.
Fierer, N., Bradford, M. A., and Jackson, R. B., 2007, Toward an ecological classification of soil bacteria: Ecology, v. 88, no. 6, p. 1354–1364.
Fuller, A. J., Shaw, S., Peacock, C. L., Trivedi, D., and Burke, I. T., 2016, EXAFS study of Sr sorption to illite, goethite, chlorite, and mixed sediment under hyperalkaline conditions: Langmuir: The ACS Journal of Surfaces and Colloids, v. 32, no. 12, p. 2937–2946.
Geszvain, K., Butterfield, C., Davis, R., Madison, A., Lee, S., Parker, D., Soldatova, A., Spiro, T., Luther, G., and Tebo, B., 2012, The molecular biogeochemistry of manganese(II) oxidation: Biochemical Society Transactions, v. 40, no. 6, p. 1244–1248.
Gillieson, D. S., 2011, Management of caves, *in* van Beynen, P., ed., Karst Management: New York, Springer, p. 141–158.
Hammer, Ø., Harper, D. A. T., and Ryan, P. D., 2001, PAST: Paleontological statistics software package for education and data analysis (version 3.12): Palaeontologia Electronica, v. 4, no. 1, p. 9.
Hansel, C. M. and Learman, D. R., 2016, The geomicrobiology of manganese: *in* Ehrlich, H. L., Newman, D. K., and Kappler, A., eds., Ehrlich's Geomicrobiology (6th edition): CRC Press, p. 401–452.
Hartmann, A., Goldscheider, N., Wagener, T., Lange, J., and Weiler, M., 2014, Karst water resources in a changing world: Review of hydrological modeling approaches: Reviews of Geophysics, v. 52, no. 3, p. 218–242.
Hasenmueller, E. A., Baraza, T., Hernandez, N. F., and Finegan, C. R., 2023, Cave sediment sequesters anthropogenic microparticles (including microplastics and modified cellulose) in subsurface environments: Science of the Total Environment, v. 893, p. 164690.
Hatcher, R. D. Jr., Lemiszki, P. J., and Whisner, J. B., 2007, Character of rigid boundaries and internal deformation of the southern Appalachian foreland fold-thrust belt, *in* Sears, J. W., Harms, T. A., and Evenchick, C. A., eds., Whence the Mountains? Inquiries into the Evolution of Orogenic Systems: A Volume in Honor of Raymond A. Price: Geological Society of America Special Paper 433, Geological Society of America, p. 243–276, https://doi.org/10.1130/2007.2433(12).
He, Y., Li, J., Li, X., Liao, J., Liang, Q., Li, H., Duan, R., Wang, C., Liu, B., Xue, Y., and Li, T., 2024, Characteristics and influencing factors of dissolved organic matter in cave drip water—a case study from Furong Cave, southwest China: Water, v. 16, no. 2, p. 207–222.
Heip, C., 1974, A new index measuring evenness: Journal of the Marine Biological Association of the United Kingdom, v. 54, no. 3, p. 555–557.
Hutchens, E., Gleeson, D., McDermott, F., Miranda-CasoLuengo, R., and Clipson, N., 2010, Meter-scale diversity of microbial communities on a weathered pegmatite granite outcrop in the Wicklow Mountains, Ireland; Evidence for mineral induced selection?: Geomicrobiology Journal, v. 27, no. 1, p. 1–14.
Kosznik-Kwaśnicka, K., Golec, P., Jaroszewicz, W., Lubomska, D., and Piechowicz, L., 2022, Into the unknown: microbial communities in caves, their role, and potential use: Microorganisms, v. 10, no. 2, p. 222.
Krumbein, W. E. and Altmann, H. J., 1973, A new method for the detection and enumeration of manganese oxidizing and reducing microorganisms: Helgoländer Wissenschaftliche Meeresuntersuchungen, v. 25, no. 2–3, p. 347–356.
Kulander, B. R. and Dean, S. L., 1986, Structure and tectonics of central and southern Appalachian valley and ridge and plateau Provinces, West Virginia and Virginia: AAPG Bulletin, v. 70, no. 11, p. 1674–1684.
Lamprinou, V., Danielidis, D. B., Pantazidou, A., Oikonomou, A., and Economou-Amilli, A., 2014, The show cave of Diros vs. wild caves of Peloponnese, Greece-distribution patterns of Cyanobacteria: International Journal of Speleology, v. 43, no. 3, p. 335–342.

Lange-Enyedi, N. T., Borsodi, A. K., Németh, P., Czuppon, G., Kovács, I., Leél-Őssy, S., Dobosy, P., Felföldi, T., Demény, A., and Makk, J., 2023, Habitat-related variability in the morphological and taxonomic diversity of microbial communities in two Hungarian epigenic karst caves: FEMS Microbiology Ecology, v. 99, no. 12, p. 1–17.

Lozano, R. P. and Rossi, C., 2012, Exceptional preservation of Mn-oxidizing microbes in cave stromatolites (El Soplao, Spain): Sedimentary Geology, v. 255–256, p. 42–55.

Ma, L., Huang, X., Wang, H., Yun, Y., Cheng, X., Liu, D., Lu, X., and Qiu, X., 2021, Microbial interactions drive distinct taxonomic and potential metabolic responses to habitats in karst cave ecosystem: Microbiology Spectrum, v. 9, no. 2, p. e01152–01121.

Martin-Pozas, T., Ghezzi, D., D'Angeli, I. M., Madonia, G., Chiarini, V., Vattano, M., De Waele, J., Cappelletti, M., Saiz-Jimenez, C., and Jurado, V., 2025, Microbial and geochemical variability in sediments and biofilms from Italian Gypsum Caves: Microbial Ecology, v. 88, no. 1, p. 1–19.

McLaren, M. R. and Callahan, B. J., 2021, Silva 138.1 prokaryotic SSU taxonomic training data formatted for DADA2 [data set]: Zenodo.

McMurdie, P. J. and Holmes, S., 2013, phyloseq: an R package for reproducible interactive analysis and graphics of microbiome census data: PLoS ONE, v. 8, no. 4, p. e61217.

Montañez, I. P. and Read, J. F., 1992, Eustatic control on early dolomitization of cyclic peritidal carbonates: evidence from the Early Ordovician Upper Knox Group, Appalachians: Geological Society of America Bulletin, v. 104, no. 7, p. 872–886.

Mulec, J and Kosi, G., 2009, Lampenflora algae and methods of growth control: Journal of Cave and Karst Studies, v. 71, p. 109–115.

Mulec, J., Pašić, L., and Oarga-Mulec, A., 2025, Metabolic traits of sediment bacteria in karst caves in the light of environmental changes: Frontiers in Microbiology, v. 16, p. 1724116.

Mussman, W and Read, J., 1986, Sedimentology and development of a passive-to-convergent-margin unconformity: Middle Ordovician Knox unconformity, Virginia Appalachians: Geological Society of America Bulletin, v. 97, no. 3, p. 282–295.

Nicolosi, G., Mammola, S., Verbrugge, L., and Isaia, M., 2023, Aliens in caves: the global dimension of biological invasions in subterranean ecosystems: Biological Reviews, v. 98, no. 3, p. 849–867.

Northup, D. E., 2011, Managing microbial communities in caves, *in* van Beynen, P., ed., Karst Management: New York, Springer, p. 225–240.

Northup, D. E., Barns, S. M., Yu, L. E., Spilde, M. N., Schelble, R. T., Dano, K. E., Crossey, L. J., Connolly, C. A., Boston, P. J., Natvig, D. O., and Dahm, C. N., 2003, Diverse microbial communities inhabiting ferromanganese deposits in Lechuguilla and Spider Caves: Environmental Microbiology, v. 5, no. 11, p. 1071–1086.

Norvell, B. G., 2023, The effects of substrate geochemistry on the distribution of manganese oxidizing bacteria in caves of the Upper Tennesee River Basin [MS thesis]: Boone, NC, Appalachian State University, 55 p.

Oksanen, J., Kindt, R., Legendre, P., O'Hara, B., Stevens, M. H. H., Oksanen, M. J., and Suggests, M., 2007, The vegan package: Community Ecology Package, v. 10, no. 719, p. 631–637.

Ostapenko, G., Tarashchan, A., and Mitsyuk, B., 2007, Rutile-quartz geothermobarometer: Geochemistry International, v. 45, no. 5, p. 506–508.

Piccardo, M and Bevilacqua, S., 2024, Lost in the dark: Current evidence and knowledge gaps about microplastic pollution in natural caves: Environments, v. 11, no. 11, p. 238–220.

Pipan, T and Culver, D., 2013, Forty years of epikarst: what biology have we learned?: International Journal of Speleology, v. 42, no. 3, p. 215–223.

Pronk, M., Goldscheider, N., and Zopfi, J., 2007, Particle-size distribution as indicator for fecal bacteria contamination of drinking water from karst springs: Environmental Science & Technology, v. 41, no. 24, p. 8400–8405.

Pronk, M., Goldscheider, N., Zopfi, J., and Zwahlen, F., 2009, Percolation and particle transport in the unsaturated zone of a karst aquifer: Groundwater, v. 47, no. 3, p. 361–369.

Ramette, A., 2007, Multivariate analyses in microbial ecology: FEMS Microbiology Ecology, v. 62, no. 2, p. 142–160.

Riley, A.-M., 2024, Human impact in Appalachian cave systems: How anthropogenic presence leads to the deposition of microplastics and alteration of native microbial cave communities [MS thesis]: Boone, NC, Appalachian State University, 53 p.

Saiz-Jimenez, C., 2012, Microbiological and environmental issues in show caves: World Journal of Microbiology and Biotechnology, v. 28, no. 7, p. 2453–2464.

Smoot, J. P. and Southworth, S., 2014, Volcanic rift margin model for the rift-to-drift setting of the late Neoproterozoic-early Cambrian eastern margin of Laurentia: Chilhowee Group of the Appalachian Blue Ridge: Geological Society of America Bulletin, v. 126, no. 1–2, p. 201–218.

Tebo, B. M., Clement, B. G., and Dick, G. J., 2007, Biotransformations of manganese, *in* Hurst, C. J., Crawford, R. L., Garland, J. L., Lipson, D. A., Mills, A. L., and Stetzenbach, L. D., eds., Manual of Environmental Microbiology: Washington, DC, ASM Press, p. 1223–1238.

Tebo, B. M., Johnson, H. A., McCarthy, J. K., and Templeton, A. S., 2005, Geomicrobiology of manganese(II) oxidation: Trends in Microbiology, v. 13, no. 9, p. 421–428.

Thigpen, J. R., Moecher, D. P., Stowell, H. H., Merschat, A., Hatcher, R. D., Jr, Powell, N. E., Spencer, B. M., Mako, C. A., Bollen, E. M., and Kylander-Clark, A., 2022, Defining the timing, extent, and conditions of Paleozoic metamorphism in the southern Appalachian Blue Ridge terranes of Tennessee, North Carolina, and northern Georgia: Tectonics, v. 41, no. 10, p. e2022TC007406.

Thomas, F., Hehemann, J.-H., Rebuffet, E., Czjzek, M., and Michel, G., 2011, Environmental and gut bacteroidetes: the food connection: Frontiers in Microbiology, v. 2, p. 93.

Tomczyk-Żak, K and Zielenkiewicz, U., 2016, Microbial diversity in caves: Geomicrobiology Journal, v. 33, no. 1, p. 20–38.

Turrini, P., Chebbi, A., Riggio, F. P., and Visca, P., 2024, The geomicrobiology of limestone, sulfuric acid speleogenetic, and volcanic caves: basic concepts and future perspectives: Frontiers in Microbiology, v. 15, p. 1370520.

Virginia Division of Mineral Resources, 1993, Geologic Map of Virginia: Virginia Division of Mineral Resources, scale 1:500,000: Association of American State Geologists.

von Jackowski, A., Becker, K. W., Wietz, M., Bienhold, C., Zäncker, B., Nöthig, E. M., and Engel, A., 2022, Variations of microbial communities and substrate regimes in the eastern Fram Strait between summer and fall: Environmental Microbiology, v. 24, no. 9, p. 4124–4136.

Wickham, H., 2011, ggplot2: WIREs Computational Statistics, v. 3, no. 2, p. 180–185.

Yu, H and Leadbetter, J. R., 2020, Bacterial chemolithoautotrophy via manganese oxidation: Nature, v. 583, no. 7816, p. 453–458.

Zhong, L., Deng, J., Song, Z., and Ding, P., 2011, Research on environmental impacts of tourism in China: Progress and prospect: Journal of Environmental Management, v. 92, no. 11, p. 2972–2983.